Surface Area Evolution of Calcium Hydroxide During Calcination and Sintering

A simple one-dimensional mathematical model validated with high-temperature entrained-flow reactor data successfully explained dispersed calcium hydroxide particle surface area evolution resulting from concomitant calcination and sintering. An integrated first-order calcination rate expression and a second-order sintering rate form accurately predicted time-resolved surface area generation and degradation. The effects of water vapor and gaseous carbon dioxide concentration on asymptotic specific surface areas and sintering rates were noted. This methodology for predicting sorbent surface area evolution will enable more accurate sulfation modeling efforts in furnace sorbent injection (FSI) applications, where calcination, sintering, and sulfation can all occur on the same time scale.

M. C. Mai
Research and Development Department
Consolidation Coal Company
Library, PA 15129

T. F. Edgar
Department of Chemical Engineering
University of Texas
Austin, TX 78712

Environmental considerations and the high cost of flue-gas desulfurization (FGD) have continually plagued the economics of utility and industrial applications of coal-fired boilers. The recent disclosure of the potential link between SO_2 and NO_x emissions and acid rain may result in the necessity of introducing more stringent regulations to control these two pollutants. There has been great interest in the high-temperature entrained-flow application, where calcium oxide reacts with gaseous sulfur dioxide, because of the potential for cost-effective reduction of SO_2 emissions from pulverized coal combustors. Furnace sorbent injection (FSI) is an emerging technology, predicated on the ability of calcium-based sorbents to scavenge sulfur from flue gas, offering a potentially viable alternative to the high cost of traditional FGD.

The dependence of apparent sorbent reactivity on calcine specific surface area has been addressed by others (Simons and Garman, 1986; Simons et al., 1987; Borgwardt and Bruce, 1986). However, much of the previous work has used extremely simplified interpretations of the phenomena involved, namely the simultaneous occurrence of calcination and sintering. Previous FSI modeling efforts (Bortz et al., 1986; Silcox et al., 1986; Bobman et al., 1985; Simons and Garman, 1986) assumed that the calcination rate was instantaneous or experimentally excluded this effect by using precalcines. Similarly, sintering has been disregarded in some studies by using presintered particles. Other investigations have employed assumptions about the kinetics that are not justified adequately.

More recent work has suggested that calcination, sintering, and sulfation may all occur on the same time scale (Newton and Pershing, 1986; Newton et al., 1985; Mai, 1987). Previous models have not considered that all three processes occur simultaneously. In addition, limited studies have suggested the potential for accelerated sintering rates and reduced asymptotic specific surface areas for calcines in the presence of water vapor and carbon dioxide at levels typically found in coal combustors (Borgwardt and Bruce, 1986; Bortz et al., 1986; Borgwardt et al., 1986; Newton et al., 1985). $CaSO_4$ has also been shown to accelerate CaO surface area reduction (Glasson, 1967). The influence of these two gas species on sintering is not well quantified at present.

This paper is a theoretical and experimental effort aimed at resolving some of the causal relationships involved in the complex process governing calcium oxide specific surface area evolution. A simple transient model is proposed that utilizes first-order calcination kinetics and a second-order sintering rate form to explain time-resolved surface area data for calcium hydroxide injected into a high-temperature entrained-flow reactor. Isothermal studies using reagent-grade calcium hydroxide particles with a mass median particle diameter of 12.5 μm and specific surface areas of 11.5 m^2/g were performed at 1,275 and 1,425 K with residence times of 0.1 to 3.5 s. In addition to testing with 100% nitrogen sweep gas, various CO_2 and H_2O levels in nitrogen were studied.

Experimental

A variety of studies have been performed investigating calcination and sintering in differential reactors, fixed-bed reactors,

and thermal gravimetric analyzers. In this investigation, however, every effort was made to replicate the entrained-flow conditions that particles would experience in FSI applications. Here, Sherwood numbers approach 2.0 for small spherical particles and mass as well as heat transfer limitations may become important. This is true for calcination and sintering rates, both of which may be affected by local gas concentrations.

The goal of the experimentation was to test the validity of proposed rate forms for calcination and sintering in this type of environment and to establish the time and temperature regimes (if they exist) that should be accounted for in future FSI modeling. An attempt was also made to investigate the influence and relative importance of CO_2 and water vapor on "catalyzed" surface area reductions.

The basic experimental apparatus consisted of a high-temperature entrained-flow reactor, a product quench and cleanup system, a data acquisition and control system, and coolant, process gas, and solids feed systems. A detailed description of the experimental design has been presented elsewhere (Mai, 1987). A schematic of the reactor is shown in Figure 1.

A fluidized-bed feeder (modified from Hamor and Smith, 1971) was used to establish steady feed rates of micron-size particles. A schematic of the sorbent feeder is shown in Figure 2. Reagent-grade calcium hydroxide (MMD = 12.5 μm) was utilized instead of commercial materials due to ease in sustaining constant feed rates in the range of 10–30 mg/min. Solids offtake rates were maintained at levels providing injection point velocities as close as possible to the reactor center-line velocity. Thus, stable laminar flow without jetting was achieved.

Approximately 2 to 5 SLPM of product gas was passed through the sample loop. Product gases were quenched to 600–650 K in about 50 ms as they passed through the air-cooled sample probe. Particulates were retained on a quartz wool substrate packed in a heated 3.6 cm O.D. tube maintained at 575 K. This sampling temperature was chosen based on constraints of minimizing carbonation and limiting continued dehydroxylation (or subsequent rehydration). Sampling integrity experiments revealed less than 5% combined carbonation/rehydration over the range of entrainment gas compositions tested. The gaseous products were then cooled to 420 K and were passed through a hygroscopic exchange membrane for the selective removal of water vapor. The cool, clean, dry product gases were sampled by a Horiba PIR-2000 infrared CO_2 analyzer and vented to atmosphere.

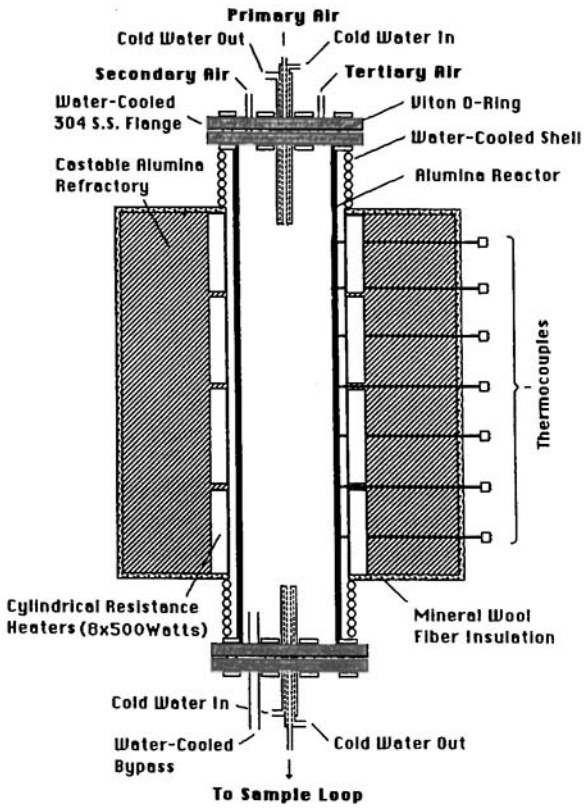

Figure 1. High-temperature entrained-flow reactor.

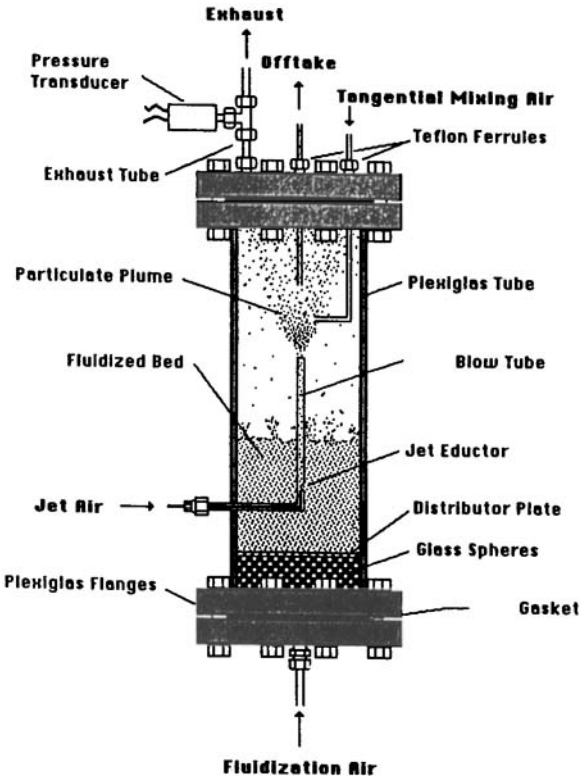

Figure 2. Fluidized bed sorbent feeder.

Calcination runs were performed under entrained-flow conditions to directly observe rates of dehydroxylation for calcium hydroxide at high temperatures. One goal was to validate the assumed first-order Arrhenius expression and to determine the apparent activation energy. Calcium hydroxide particles were partially calcined for a variety of residence times at two different temperatures (1,275 and 1,425 K). The procedure followed to obtain these samples required establishment of isothermal conditions in the reactor, and setting flow rates and probe positions to achieve the desired residence times.

Solids feed rates were usually set around 10–30 mg/min. This provided gas/solid loading ratios of 500 to 1 on a mass basis. Hot solid samples were purged with cool nitrogen, removed from the solids sampling tube, and placed immediately in sample bottles under dry air. New quartz wool was inserted and the sampling tube was reattached. Solids samples were taken every 5 minutes for a duration of 10 to 90 minutes, stopping when approximately 300 mg of partially calcined sorbent were

acquired. The total time required for an individual run depended on the relative positioning of the sample and injection probes, the gas flow rate through the sampling loop, and the solids feed rate.

Particle residence times were determined using laminar flow center-line velocities and calculated particle terminal velocities. Stokes law was used to calculate drag coefficients as particle Reynolds numbers were substantially less than 1.0.

Solid samples were analyzed for fractional calcination using a Varian AA-1475 Series Atomic Spectrophotometer. An acetylene-nitrous oxide flame was used in conjunction with a 10 mA calcium lamp. The instrument was calibrated at a wavelength of 422.7 nm using mixtures of 0.0, 2.0 and 4.0 ppm Ca in 0.2 M NaOH. Samples were weighed and then diluted in 50 mL of distilled H_2O. Successive dilution trials were then performed until a calcium solution of approximately 4.0 μg/mL was obtained. Three 20-second sample runs were then averaged and the percentage of calcium in the original sample was computed. The fractional conversion was calculated recognizing that $Ca(OH)_2$ is 54.10% Ca and CaO is 71.47% Ca on a mass basis.

Sintering tests were performed to validate rate forms used in the sorbent surface area evolution model and to determine Arrhenius rate parameter values. Additionally, the effects of CO_2 and H_2O concentration on the sintering process were evaluated.

Sintering tests performed with a nitrogen sweep gas followed the same procedure described for the calcination experiments. Carbon dioxide was also injected into the sweep gas and for H_2O tests the feed mixture passed through an evaporator system with temperature control to set H_2O concentrations. Calcine specific surface areas were examined by nitrogen adsorption at -195°C using a Micromeritics Model 2100D Analyzer. Specific surface areas were determined using the method of Brunauer, Emmett, and Teller (1938).

Sorbent Surface Area Evolution Model

Calcination rates for limestone have been presented as first-order Arrhenius expressions in previous investigations (Beruty and Searcy, 1974; Borgwardt, 1985). Sintering effects on precalcines have been described by two-parameter Arrhenius relationships with the rate proportional to the difference between the specific surface area and an asymptotic specific surface area squared (Bortz et al., 1986; Silcox et al., 1986). The following is an extension of these investigations applied to the simultaneous calcination and sintering of $Ca(OH)_2$.

The previously mentioned rate form for calcination of $CaCO_3$ was extended to the calcination of calcitic hydrates. The rate of conversion may be expressed as,

$$\frac{dm_h}{dt} = -k_c S_h m_h \tag{1}$$

where the hydroxide surface area is equal to the specific surface area (S_h) times the mass of calcium hydroxide (m_h). The calcination rate may be expressed as an Arrhenius form.

$$k_c = A_c e^{-E_{a,c}/RT} \tag{2}$$

An expression relating conversion and time can be obtained by integrating Eq. 1,

$$\ln (1 - X) = -k_c S_h t \tag{3}$$

Borgwardt reported calcined specific surface areas in the absence of sintering in the range of 70–80 m^2/g. This initially high surface area calcine then sinters, approaching a surface area of S_a. Previous investigations with precalcines have indicated second-order kinetics (Bortz et al., 1986; Silcox et al., 1986; Cole et al., 1986). Therefore, letting τ represent the age of discrete CaO grains, the sintering rate may be expressed as,

$$\frac{dS_c}{d\tau} = -k_s(S_c - S_a)^2 \tag{4}$$

where the rate constant is described by,

$$k_s = A_s e^{-E_{a,s}/RT} \tag{5}$$

and S_c is the time-dependent CaO specific surface area. Integration provides an expression for S_c as a function of age and the initial (S_i) and asymptotic calcine specific surface areas (S_a).

$$S_c = \frac{1}{k_s\tau + \dfrac{1}{S_i - S_a}} + S_a \tag{6}$$

At any time t_p the fractional conversion of the hydroxide X_p may be calculated using Eq. 3. Specifying the time also fixes the complete distribution of CaO grain ages. A relationship describing the fraction of the calcine y with age τ at a point in time t_p is required. Moving from the time domain into the age (integrated time) domain yields,

$$y = \frac{X_p - X}{X_p} \tag{7}$$

and

$$\tau = t_p(1 - t/t_p) \tag{8}$$

Using these relationships and Eq. 3 leaves,

$$\ln (1 - X_p(1 - y)) = -k_c S_h (t_p - \tau) \tag{9}$$

Now solving for τ,

$$\tau = \frac{k_c S_h t_p + \ln (1 - X_p(1 - y))}{k_c S_h} \tag{10}$$

The expression for τ may now be substituted back into Eq. 6,

$$S_c = S_a + \left\{ k_s \left[\frac{k_c S_h t_p + \ln [1 - X_p(1 - y)]}{k_c S_h} \right] + \frac{1}{S_i - S_a} \right\}^{-1} \tag{11}$$

The average CaO specific surface area may now be represented as,

$$\bar{S}_c = \int_0^1 S_c \, dy \tag{12}$$

The average specific surface area of the sorbent particle is then

a combination of the contributions of both the uncalcined $Ca(OH)_2$ and the CaO,

$$S_s = (X)\bar{S}_c + (1 - X)S_h \quad (13)$$

where S_s is the sorbent particle specific surface area. The sorbent particle specific surface area can thus be expressed as a function of time, initial $Ca(OH)_2$ specific surface area, and initial and asymptotic calcine specific surface areas.

Nitrogen Sweep Gas Results

Calcination experiments using reagent grade $Ca(OH)_2$ were performed at 1,275 and 1,425 K to establish rate parameters and to validate the first-order rate form used in the calcination/sintering model. Figure 3 is a plot of the experimental calcination results at these two temperatures. The rate constants were established by minimizing the sum of the squares of the error between fitted and experimental values. The activation energy and preexponential factor were then calculated based on these determinations.

The calcination runs at 1,275 K produced a value for k_c of 0.22 g/m^2 · s. This compares to the result of 0.43 g/m^2 · s for the 1,425 K runs. The calculated apparent activation energy was 68.3 kJ/mol. This is lower than the value of 116 kJ/mol reported by Criado and Morales (1976) and reflects the significance of heat and mass transfer limitations in the entrained-flow system. Measurable dehydroxylation of the $Ca(OH)_2$ particles was not observed under residence times of 0.1 s. Therefore, this heatup time lag was subtracted from residence times while calculating calcination rates. The first-order Arrhenius rate expression does appear to accurately match the experimental results.

More recent work has established the importance of sorbent/gas mixing in determining sulfation rates. The calcination rates reported here are an order of magnitude lower than some of the recent literature values and, although applicable, may not represent optimal conversions.

Sintering experiments were performed at 1,285 and 1,425 K to validate the rate form used in the calcination/sintering model and to determine required rate parameters. The second-order Arrhenius expression presented previously requires both a knowledge of the rate constant and the sintered asymptotic specific surface area. Nonlinear regression was used to determine the rate constants and asymptotic surface areas for both temperatures tested.

Figure 4 is a plot of simultaneous calcination and sintering in a nitrogen entrained-flow environment at 1,285 K. The calcination rate appears to dominate the sintering rate for approximately 0.3 s. The rate of generation of high surface area calcine then slows according to the first-order calcination expression. The sintering of most of the CaO grains forces a rapid surface area decline toward the asymptotic value.

The model comparisons shown are based on both the calcination rate parameters determined previously, and the results of nonlinear regressions used to fit the sintering rate constant and asymptotic surface area at 1,285 K. The calcination/sintering model was coupled to a nonlinear equation solver, and the method of Levenberg-Marquardt was used to minimize the sum of squares using two fitted parameters. The unconstrained optimization was augmented with a penalty function to prevent searches in negative parameter space. Additional fits were attempted using the calcination rate as a third adjustable parameter.

The results of the parameter estimation calculations yielded a rate constant at 1,285 K of 1.28×10^{-1} g/m^2 · s and an asymptotic surface area of 20.2 m^2/g. In minimizations performed for

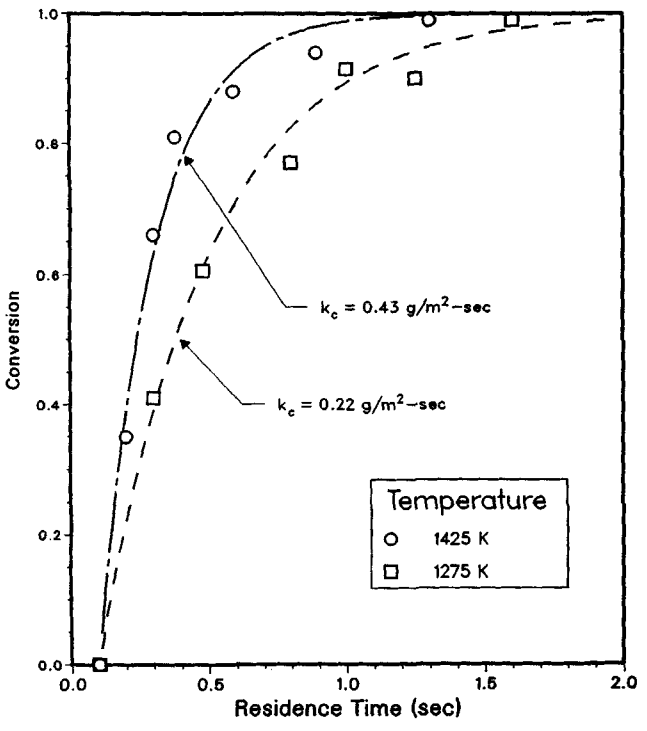

Figure 3. Effect of temperature on calcination.

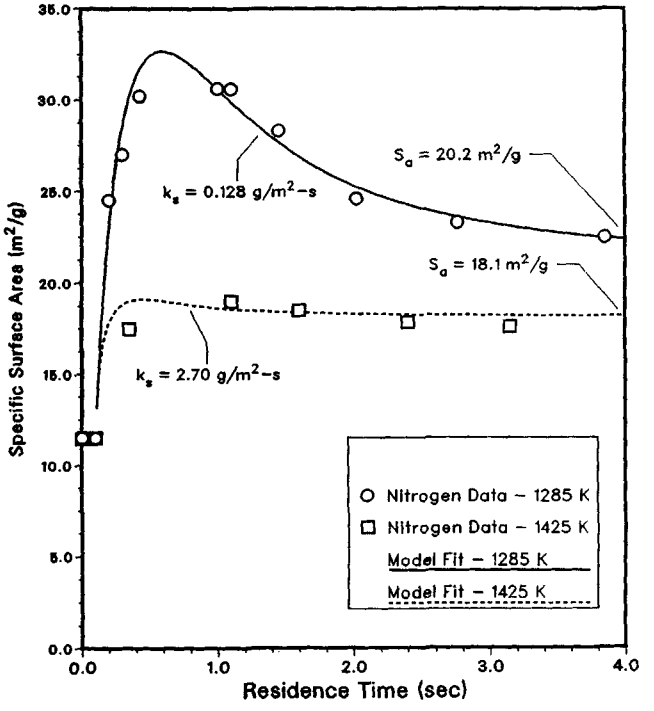

Figure 4. Effects of simultaneous calcination and sintering on surface area evolution.

three parameters (k_c, k_s, S_a), the fitted calcination rate constant was only 3.2% below the value obtained from the calcination experiments, thus providing additional validity to the second-order sintering rate form used.

A plot of sintering test results obtained at 1,425 K is also shown in Figure 4. The temperature-induced increase in calcination rate apparently did not match the accompanying rise in the sintering rate, and only a slight maximum was observed. The sintering rate parameters were determined using the same nonlinear optimization techniques previously discussed. The resulting sintering rate constant was 2.7 $g/m^2 \cdot s$, and the asymptotic surface area was determined as 18.1 m^2/g. The apparent activation energy (based only on two temperatures) was 327 kJ/mol. This compares to a value of 244 kJ/mol reported by Bortz et al. (1986).

Effects of Carbon Dioxide and Water Vapor

A factorial test matrix was used to investigate CO_2 and H_2O concentration effects on the sintering of $Ca(OH)_2$ derived CaO. These two gas species were tested at two levels each and at two different temperatures (1,285 and 1,425 K). H_2O concentrations of 4.0 and 8.0 vol.% and CO_2 concentrations of 13.0 and 18.0 vol.% were examined in an attempt to quantify sintering behavior over a range of possible coal combustion flue gas compositions.

The calcination and sintering behavior of reagent grade $Ca(OH)_2$ in nitrogen entrainment gas with 13.0 and 18.0 vol.% CO_2 is shown in Figure 5. The sintering associated with the inclusion of 13 vol.% CO_2 in the nitrogen entrainment gas at 1,285 K resulted in a 34% decrease in the peak surface area and an accompanying 5% decrease in asymptotic specific surface area.

Sintering behavior for the 18% CO_2 entrainment gas did not differ substantially from the 13% CO_2 data. The resulting surface areas were only a few percent lower for the 38.5% increase in CO_2 concentration. An additional 2% decrease in asymptotic surface area was observed and is equivalent to a 7% reduction from the baseline nitrogen-only data.

Similar surface area reductions were observed for CO_2 at 1,425 K. A 28.7% reduction in peak surface areas was observed for both the 13% and 18% tests when compared to the value of 18.1 m^2/g obtained for sintering in a 100% nitrogen sweep gas. Reductions in observed asymptotic surface areas of approximately 21 and 23% were observed for the 13 and 18% CO_2 tests, respectively. This reduction is significantly greater than those observed with the lower temperature tests.

The surface area evolution of calcium hydroxide at 1,285 and 1,425 K was also observed in the presence of 4 and 8 vol.% H_2O. A plot of sorbent specific surface area vs. residence time for sintering in 4% H_2O-96% N_2 entrainment gas is shown in Figure 6. The results are almost identical to the 13% CO_2 experiments despite the difference in gas concentrations. The 4% H_2O data, however, displayed a further 5% decrease in the asymptotic specific surface area. The similarity to CO_2-induced sintering behavior may also be extended to the 8% H_2O in nitrogen results shown. The surface areas obtained using the 18% CO_2–82% N_2 entrainment gas were matched very closely with the behavior exhibited by the $Ca(OH)_2$ particles sintered in the 8% H_2O–92% N_2 feed mixture.

Whereas behavioral similarities exist for the CO_2 and H_2O sintering results at 1,285 K, this phenomenon was not observed at 1,425 K. The resultant surface areas were approximately 7% higher for the 4% H_2O entrainment gas than for the 13% CO_2 mixture. Conversely, Figure 6 illustrates a 14% lower asymptotic surface area for the 8% H_2O tests when compared to the 18% CO_2 experiments. Apparently, the sintering process was affected more by differences in H_2O concentrations at the

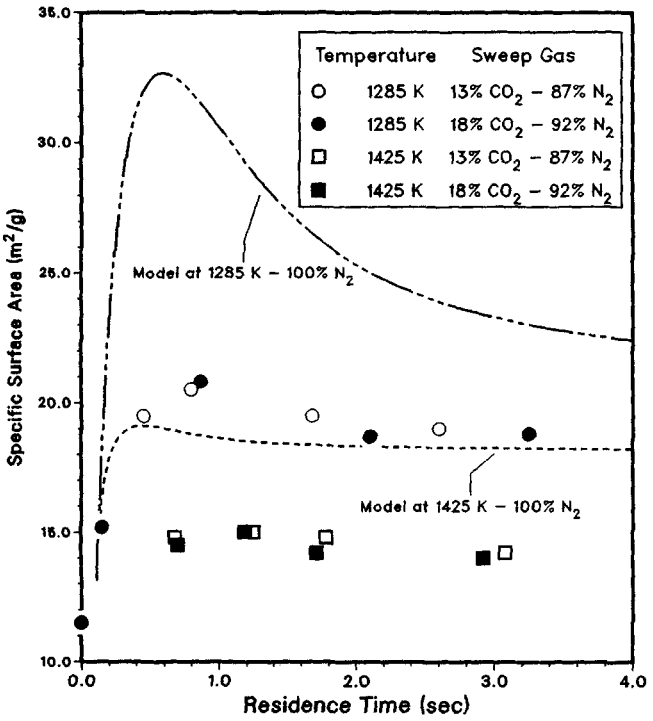

Figure 5. Simultaneous calcination and sintering in CO_2.

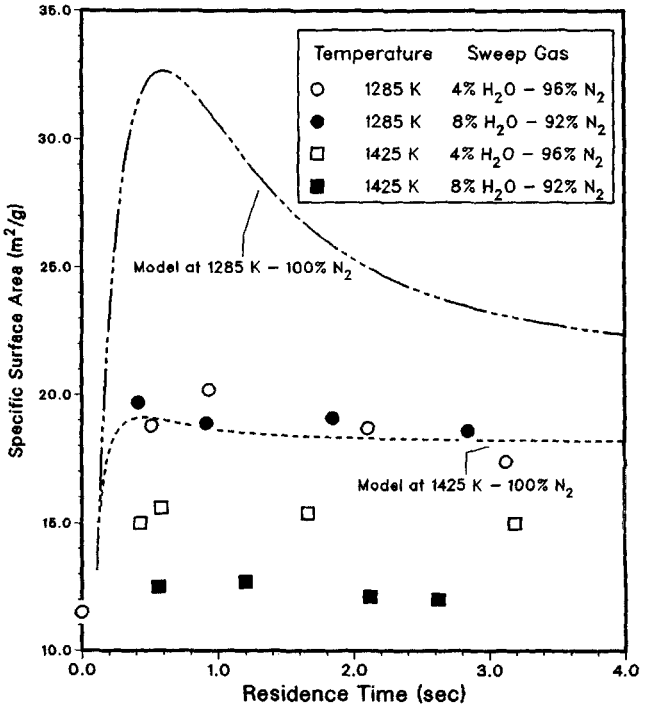

Figure 6. Simultaneous calcination and sintering in H_2O.

higher temperature tested. Additionally, the magnitude of the sintering rate overwhelms any differences that may be present in the dehydroxylation rate due to the presence of water vapor.

Experiments were also performed to evaluate the combined effects of H_2O and CO_2 on the asymptotic surface areas produced during sintering. Three replicate tests were performed for each sweep gas combination. A compilation of the test result means is shown in Figure 7.

Several trends are evident in the results. The H_2O concentration had the most effect on asymptotic surface areas, with increased CO_2 concentrations in the entrainment gas reducing these surface areas still further. The average effect of increasing the H_2O concentration from 4 to 8% was a decrease in the asymptotic specific surface area by approximately 10%. The effect of CO_2 concentration on sintering in the presence of water vapor seemed to be greater at the lower temperatures tested.

The implications of the CO_2/H_2O sintering results are understood best by recognizing the proportional relationship between surface area and sulfation potential. Although complicated by diffusional limitations, the relative differences in asymptotic specific surface areas for the calcines sintered in different CO_2/H_2O entrainment gases strongly reflect possible differences in calcium utilization during the sulfation process. This provides an alternative explanation of differing SO_2 reductions in pilot-scale testing where FSI was simulated with natural gas firing followed by coal firing (in order to determine ash interaction effects). Calcium utilizations may be fuel-specific and dependent on the concentrations of CO_2 and water vapor produced during the combustion process.

Conclusions

Bench-scale surface area data for reagent grade calcium hydroxide undergoing simultaneous calcination and sintering were developed for two temperatures, and a mathematical model based on first-order calcination kinetics and a second-order sintering rate form accurately described the time-resolved data. At the higher temperature studied (1,425 K) surface area evolution was dominated by the calcination rate with a very rapid increase in generated specific surface area. After the occurrence of a slight maximun in surface area, a degradation toward a temperature- and concentration-dependent asymptotic value resulted. At the lower temperature, the calcination and sintering rates were of the same magnitude, and a stronger surface area peak for early residence times was observed.

Water vapor concentration had the largest effect on asymptotic surface areas, with increased CO_2 concentrations in the entrainment gas reducing these surface areas still further. Inclusion of the two gas species in the sweep gas also accelerated the sintering rates and resulted in a smoothing of the surface area maxima in the time-resolved data.

This research has important implications for FSI modeling. Recognizing the direct dependence of sulfation rate on calcine specific surface area, a significant improvement in the accuracy of future sulfation modeling will result if concurrent calcination and sintering at moderate FSI temperatures are taken into account. These effects are somewhat reduced at higher temperatures where calcination is rapid and surface areas quickly approach asymptotic values. Moreover, the variation in observed asymptotic surface area ratios for $N_2/CO_2/H_2O$ entrainment-gas mixtures implies a site-specific sulfation potential dependent on the concentration of these species in the flue gas.

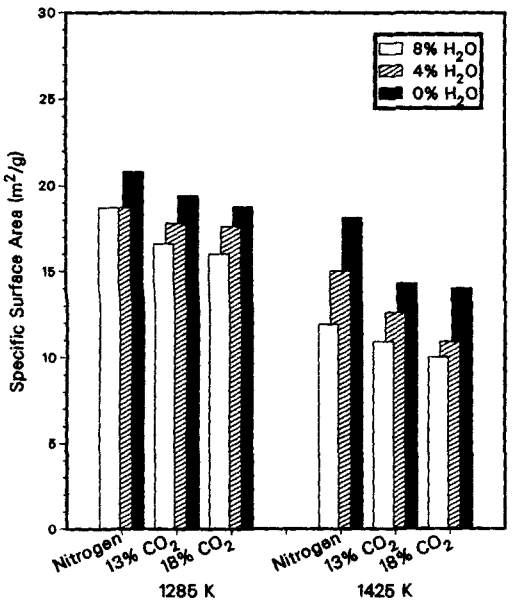

Figure 7. Effect of sweep gas composition on asymptotic specific surface areas.

Notation

A = preexponential factor, g/m² · s
E_a = activation energy, kJ/mol
k = rate constant, g/m² · s
m = mass, g
S = specific surface area, m²/g
$\bar{S}$ = average specific surface area, m²/g
T = temperature, K
t = time, s
X = conversion of calcium hydroxide to calcium oxide
τ = age of calcium oxide grains, s

Subscripts

a = asymptotic value
c = calcium oxide
h = calcium hydroxide
i = initial value
p = arbitrary point in time
s = sorbent

Literature Cited

Beruto, D., and A. W. Searcy, "Use of Langmuir Method for Kinetic Studies of Decomposition Reactions: Calcite ($CaCO_3$)," *J. Chem. Soc. Farad. Trans.*, **7**, 2145 (1974).

Bobman, M. H., G. F. Weber, and T. C. Keener, "Additive Enhancement of Pressure Hydrate Lime for Control of SO_2/NOx Emissions," AIChE Mtg. (Mar., 1985).

Borgwardt, R. H., "Calcination Kinetics and Surface Area of Dispersed Limestone Particles," *AIChE J.*, **31**(1), 1 (Jan., 1985).

Borgwardt, R. H., and K. R. Bruce, "Effect of Specific Surface Area on the Reactivity of Calcium Oxide with SO_2," *AIChE J.*, **32**(1), 2 (Jan., 1986).

Borgwardt, R. H., N. F. Roache, and K. R. Bruce, "Method for Variation of Grain Size in Studies of Gas-Solid Reactions Involving CaO," *I. and E. C. Fund.*, 25 (1986).

Bortz, S. J., V. P. Roman, R. J. Yang, P. Flament, and G. R. Offen, "Precalcination and Its Effect on Sorbent Utilization During Upper Furnace Injection," Symp. on Dry SO_2/No_x Control Technologies, Raleigh, NC (June 2–6, 1986).

Brunauer, S., P. H. Emmett, and E. Teller, "The Adsorption of Gases in Multimolecular Layers," *J. Amer. Chem. Soc.*, **60**, 309 (1938).

Cole, J. A., J. C. Kramlich, W. R. Seeker, G. D. Silcox, G. H. Newton, D. J. Harrison, and D. W. Pershing, "Fundamental Studies of Sor-

bent Reactivity in Isothermal Reactors," Symp. on Dry SO_2/NO_x Control Technologies, Raleigh, NC (June 2–6, 1986).
Criado, J. M., and J. Morales, "On the Thermal Decomposition Mechanism for Dehydroxylation of Alkaline-Earth Hydroxides," *J. of Therm. Anal.*, **10**, 103 (1976).
Glasson, D. R., "Reactivity of Lime and Related Oxides," *J. Appl. Chem.*, **17**(4) (1967).
Hamor, R. J., and J. W. Smith, "Fluidizing Feeders for Providing Fine Particles at Low, Stable Flows," *Fuel*, **50**(4) (1971).
Mai, M. C., "Analysis of Simultaneous Calcination, Sintering and Sulfation of Calcium Hydroxide under Furnace Sorbent Injection Conditions," Ph.D. Diss., Univ. of Texas, Austin (1987).
Newton, G. H., and D. W. Pershing, "Short Time Sulfation of Porous CaO: High Temperature Experiments Compared to a Distributed Pore Model," submitted to *AIChE J.* (1986).
Newton, G. H., D. J. Harrison, G. D. Silcox, and D. W. Pershing, "Control of SOx Emissions by In-Furnace Sorbent Injection: Carbonates vs. Hydrates," AIChE Mtg., Chicago (Nov., 1985).
Silcox, G. D., R. Payne, D. W. Pershing, and W. R. Seeker, "A Comparison of Combustion Facilities and Calcium Based Sorbents in Terms of Their Sulfur Capture Performance," Symp. on Dry SO_2/NO_x Control Technologies, Raleigh, NC (June 2–6, 1986).
Simons, G. A., and A. R. Garman, "Small Pore Closure and the Deactivation of the Limestone Sulfation Reaction," *AIChE J.*, **32**(9), 1491 (Sept., 1986).
Simons, G. A., A. R. Garman, and A. A. Boni, "The Kinetic Rate of SO_2 Sorption by CaO," *AIChE J.*, **33**(2), 211 (Feb., 1987).

Manuscript received on Jan. 9, 1988, and revision received Aug. 15, 1988.